Eur. Phys. J. D (2014) 68: 127
DOI: 10.1140/epjd/e2014-50087-5

THE EUROPEAN PHYSICAL JOURNAL D

Regular Article

Positron transport in CF_4 and N_2/CF_4 mixtures*

Ana Banković[1,a], Saša Dujko[1], Srdjan Marjanović[1], Ronald D. White[2], and Zoran Lj. Petrović[1]

[1] Institute of Physics, University of Belgrade, Pregrevica 118, 11080 Belgrade, Serbia
[2] ARC Centre for Antimatter-Matter Studies, School of Engineering and Physical Sciences, James Cook University, Townsville 4810, Australia

Received 31 January 2014 / Received in final form 18 March 2014
Published online 20 May 2014 –

Abstract. In this paper we present our recently compiled set of cross sections for positron scattering in CF_4. Using this set of cross sections as an input in our multi term Boltzmann equation analysis of positron transport in CF_4 and N_2/CF_4 mixtures, we calculate various transport properties as a function of the reduced electric field E/n_0. Values and general trends of the mean energy, drift velocity and diffusion coefficients as a function of E/n_0 are reported here. Emphasis is placed on the explicit and implicit effects of positronium (Ps) formation on the drift velocity and diffusion coefficients. Two important phenomena arise. Firstly, for certain regions of E/n_0 the bulk and the flux components of the drift velocity and longitudinal diffusion coefficient are markedly different, both qualitatively and quantitatively. Secondly, and contrary to previous studies in positron swarm studies, there is negative differential conductivity (NDC) in both the bulk and flux drift velocity. The variation of the drift velocity with E/n_0 and origin of the NDC are addressed using physical arguments. Cross sections and transport data for positrons in CF_4 and N_2/CF_4 mixtures presented in this work are compiled and evaluated with an aim of improving the efficiency of positron traps.

1 Introduction

Positron physics is a growing area of research [1–3], ranging from medical science [4] and astrophysics [5] to material science [6]. The fundamental data on positron behavior in gaseous, liquid and solid matter under different conditions and in various environments are rapidly increasing and new possibilities for applications are emerging (positherapy [7,8] being an exotic example). Modeling of these applications is necessary because it can provide a better insight into the fundamental phenomena, and enable optimization of such applications. Modeling, however, usually requires two types of input data. The first are complete sets of cross sections for collisions of positrons with individual atoms and/or molecules of matter in question. The second are transport data, relying on scattering data, that are the source of information about a group or ensemble properties of positrons (swarm) traveling through the medium, such as their mean energy, drift velocity and diffusion. Unfortunately, the experimental data on transport coefficients for positrons [9] are very limited in the literature and only a few groups in the world are directly involved in modeling of positron transport. A review of the history and current status of positron swarm experiments have been recently outlined by Charlton [9] and Petrović et al. [10].

The invention of the Surko trap [11,12] has made a revolutionary breakthrough in measuring positron cross section data and provided a renewed momentum to positron physics. Before such traps, it was impossible to achieve positron beams with sufficient flux and energy resolution. Nowadays Surko traps are the main source of positrons for positron scattering experiments from atoms and molecules [13–17] and other experiments [18–21]. Those range from the creation of positronium (Ps) molecules [22] to the formation of anti-hydrogen atoms [22–24], and even experiments aiming to achieve Ps Bose-Einstein condensates [25].

The positron scattering data resulting from experiments based on the Surko trap together with the theoretical cross-section calculations have triggered a series of swarm oriented studies where calculation of transport parameters for positrons in various gases under the influence of both the electric and magnetic fields plays the central role [26–31]. Positron beams in the Surko trap evolve quickly into a 'swarm-like' particle distribution [32], so the concepts and theory of charged particle swarms are highly appropriate to model the behavior of positrons in

* Contribution to the Topical Issue "Electron and Positron Induced Processes", edited by Michael Brunger, Radu Campeanu, Masamitsu Hoshino, Oddur Ingólfsson, Paulo Limão-Vieira, Nigel Mason, Yasuyuki Nagashima and Hajime Tanuma.

[a] e-mail: ana.bankovic@gmail.com

this trap. Although the existing design of the trap currently facilitates many different kinds of measurements, it is always desirable to try to store more positrons. Modeling of the positron trap operation [32] is important in order to better understand the underlying mechanisms and improve the trapping efficiency, thermalization time and beam radius. One of the illustrative outcomes of recent simulations was a suggestion that a trap setup with CF_4 as the only trapping gas at incoming energies far below the threshold for Ps formation, will achieve higher efficiency [33].

The most efficient buffer gas in positron traps so far was N_2, with the addition of CF_4 in the final stage of the trap. The threshold for excitation of the $a^1\Pi$ electronic level of N_2 in positron impact is conveniently positioned just below the threshold for Ps formation [34]. Cross sections for these two processes are of similar magnitude, and therefore a huge percentage of positrons hit the electronic excitation, lose their energy and never get a chance to form Ps and disappear from the swarm [28]. Cooled positrons are transferred into the final stage of the trap where they collide with CF_4 molecules and lose significant amount of their energy through the vibrational excitation of CF_4 [13].

In order to calculate positron transport coefficients either by Monte Carlo simulation [35,36] or through a numerical solution of Boltzmann's equation [37,38], it is necessary to have a complete set of cross sections for positron scattering. We regard a set of cross sections which covers all important processes and provides a good balance of number of particles, momentum and energy within the swarm to be complete. In the case of electron swarms there are recommended sets for many atoms and molecules which are being revised and updated regularly, as illustrated for example in reference [39], but for positrons such data are often missing in the literature [40]. In those cases it is unavoidable sometimes to make educated guesses, for example to use available data for positron scattering with similar atoms/molecules or even data for electron scattering. The basic differences between electron and positron scattering can be summarized in the following points [1]: (i) the short-range positron-atom interaction is repulsive in contrast to the attractive electron-atom interaction; (ii) for positrons the exchange interaction does not exist; and (iii) positronium (Ps) formation channel is very strong and unique for positron interaction. Basically, the most significant differences between the positron cross sections and electron cross sections are in the low-energy range, and that is exactly the range that we are interested for in this paper. Therefore, in creating cross section sets for positrons in N_2 and CF_4, we have been forced [28,40] to carefully compile the best available data from the literature and to find the best ways to overcome the problems arising from the fundamental data that are not available.

In this paper we present our set of cross sections for positron scattering in CF_4, with the primary aim for use in modeling of cooling processes of positron cloud in the buffer gas positron accumulators. Using this set and previously developed and published set of cross sections for positron scattering in N_2 [28,40], we have calculated transport properties for positrons in pure CF_4 and in mixtures of N_2 with different percentage contribution of CF_4. One of the most important motivational factors for this work was the development of a database of collisional and transport data for the recently suggested pure CF_4 trap [33]. We believe that data presented in this paper can additionally support the ideas presented in reference [33]. Transport properties for positrons have been calculated using a multi term Boltzmann equation analysis [36–38]. A Monte Carlo simulation technique [31,36] is used as an additional method to test some of the interesting and atypical phenomena observed in the positron transport in pure CF_4 and CF_4/N_2 mixtures.

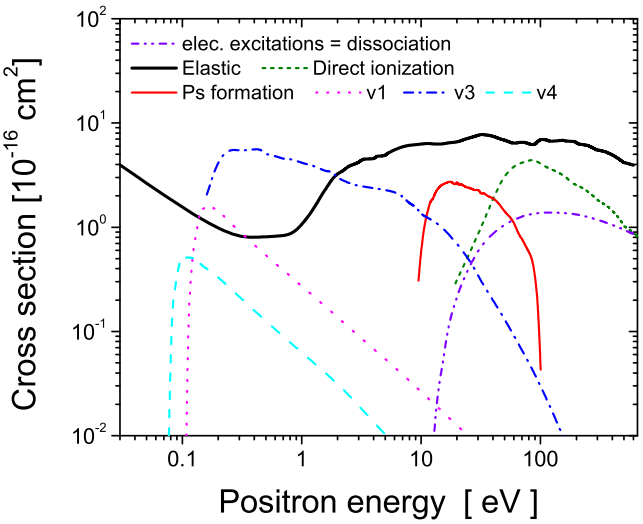

Fig. 1. Cross sections for positron scattering in CF_4.

2 Cross sections for positrons in CF_4

The cross section set for positron interactions with CF_4 is shown in Figure 1. This set includes cross sections for elastic collisions, Ps formation and inelastic processes (direct ionization, vibrational and electronic excitations). In creating this cross section set we primarily had in mind the important role that CF_4 has as a cooling gas in Surko-type positron traps [11,12]. Therefore, this 'complete set' does not include the cross section for direct annihilation since it is not relevant for the behavior of positrons in the trap [32]. Currently, CF_4 is used in the last (low energy) stage of thermalization in the Surko traps, and the approximate estimates of Ps formation, direct ionization and electronic excitation cross sections were not critical factors in the models. However, as there were suggestions that CF_4 may be used as the sole trapping gas [33], and also for rotating wall applications [21,41], we have attempted to make the set as complete as is presently possible. We hope that this will also give motivation for experimentalists and theoreticians to provide the necessary data for the missing processes.

The total cross section is taken from the experiment of Makochekanwa et al. [17] and it covers the energy range from 0.2 to 1000 eV. It is extrapolated to zero energy using the theory of Nishimura and Gianturco [42]. The elastic cross section is obtained by subtracting all inelastic cross sections and the cross section for Ps formation from the total cross section.

To our knowledge, there is no data on the Ps formation cross section for CF_4 in the literature. Therefore we have used the cross section for Ps formation in Ar (as suggested in Ref. [14]) shifted by the difference between the thresholds for this process in Ar and CF_4. The justification for this choice lies with the fact that cross sections for ionization are very similar in both shape and magnitude for Ar and CF_4. There is a new measurement of Ps formation cross section in Ar [15], which agrees in shape with [14] and slightly differs in magnitude (it is 9% higher at the peak). We believe that such a small difference will not greatly affect the positron transport data. Thresholds for Ps formation in Ar and CF_4 are 8.955 eV [14] and 9.45 eV [17], respectively, so we added $\Delta = 0.495$ eV to the energy scale of the Ps cross section for Ar. The other choice would have been the Ps formation cross section for CH_4, but to the best of our knowledge there is no Ps formation data for this molecule in the literature.

A similar situation exists for the cross section for direct ionization of CF_4 via positron impact. Our starting point in constructing this cross section was the cross section for total ionization of CF_4 (i.e. including all ionisation processes – direct and Ps-formation ionizations of the molecule) measured by Moxom et al. [43] in the energy range 6−47 eV. It was extrapolated to higher energies using the total ionization cross section for positrons in CH_4 measured by Bluhme [44], shifted by the difference between the thresholds for this process in CF_4 and CH_4. When shifted by this difference ($\Delta = 3.303$ eV), the CH_4 cross section smoothly merges with the CF_4 cross section. We then subtracted the cross section for Ps formation previously described from the obtained total ionization cross section to get the direct ionization cross section for CF_4 via positron impact. The threshold for this process is 16.25 eV. Since the most important role in positron trapping is played by the huge cross sections for vibrational excitations of CF_4 in both the Surko trap and the recently proposed CF_4 trap [33], we believe that approximate estimates of the Ps formation cross section and the cross section for direct ionization are not critical factors [13] and are sufficient for our modelling considered here.

Electronic excitations of the CF_4 molecule induced by positron impact also play an important role in enhancing the percentage of trapped particles when CF_4 is one of primary cooling gases [33]. Unfortunately, again there is a lack of data in the literature. One way to include electronic excitations into the cross section set is to take the effective cross sections for electronic dissociative excitations by electrons [45] and then to divide it by the factor of 4 [46] as positrons may only excite singlet transitions.

The most important process in the trapping of positrons in Surko trap [21,41] and in CF_4 trap [33] are vibrational excitations of CF_4. This cross section set includes cross sections for three of the four vibrational excitations [34]: v1 ($E_{exc} = 0.113$ eV), v3 ($E_{exc} = 0.159$ eV) and v4 ($E_{exc} = 0.078$ eV). The cross section for vibrational excitation v2 ($E_{exc} = 0.054$ eV) is omitted because neither experimental nor theoretical data exist for this transition, for neither positrons and electrons presumably due to its small magnitude or as it was included in one of the other three processes. The energy range relevant for this process is still apparently out of reach for modern experiments [34]. The cross section for v3 has been measured in San Diego in the 0.1−2 eV energy range [34]. The cross section for v3 excitation of CF_4 molecule by electron impact has also been measured in the same energy range and using the same apparatus. This experiment revealed that vibrational cross sections for electrons and positrons in CF_4 are similar both in shape and magnitude, and this is confirmed by calculations based on the Born approximation [34]. Consequently, we have extrapolated the cross section for the v3 vibrational mode using results for electrons obtained by a swarm method [47]. Since the positron data for the vibrational modes v1 and v4 are missing, we have used the available data for electrons [47].

According to the symmetry, CF_4 belongs to the spherical top molecules and also to cubic point group T_d. It therefore has no net dipole moment. A pure rotational spectrum cannot be observed by absorption or emission spectroscopy because there is neither permanent dipole nor quadrupole moment [48] and thus rotation may not be induced by the electromagnetic field of an incident photon. Further, the polarizability is isotropic so that a pure rotational transition cannot be observed by Raman spectroscopy [49]. Thus in all analyses for electron swarms in gaseous CF_4 and for plasma models the rotational interaction has been completely neglected [47,50,51]. Led by this we have used the same approximation for positrons, i.e. we have neglected rotational excitation. One should however bear in mind that in theoretical work of Varella et al. [52] cross sections have been calculated for rotational excitation of several transitions for electron CF_4 collision, with large changes in rotational quantum number. They used an ab initio Schwinger multichannel method in conjunction with norm-conserving pseudo-potentials. Their calculations give relatively high cross sections ($\sim 10^{-16}$ cm^2) for rotational excitations at high energies where the pure rotational energy transfer is estimated to be $\sim 10^{-5}$ eV per collision. This number is very small comparing to vibrational energy transfer. In principle electrons could excite optically forbidden transitions so the magnitude and the role of rotational excitation in highly symmetric molecules is still an open issue. Apart from the results of Varella et al. [52] to our knowledge there are no available rotationally resolved cross sections in the literature for CF_4. Therefore we did not try to take into account this interaction channel separately. In our set of cross sections rotational excitations of CF_4 by positron impact, if present, are implicitly included through elastic cross section through their inclusion in measured total cross section.

Another comment related to this issue should be made here. In case of electron transport in plasmas the mean energies are such that energy balance is dominated by vibrational excitation and the high energy tail of the velocity distribution function is determined largely by the electronic excitation. Thus taking or failing to take the rotational contribution is of little consequence. In the case of positrons, however, we are interested in thermalization and thus we need a good energy balance in the approach to the thermal energy where rotational excitation is the dominant inelastic process.

3 Theoretical methods

All information on the drift and diffusion of positrons in neutral gases is contained in the positron phase-space distribution function $f(\boldsymbol{r},\boldsymbol{c},t)$, where $\boldsymbol{r}$ represents the spatial coordinate of a positron at time t, and $\boldsymbol{c}$ denotes its velocity. The distribution function $f(\boldsymbol{r},\boldsymbol{c},t)$ is evaluated by solving Boltzmann's equation:

$$\left[\partial_t + \boldsymbol{c}\cdot\nabla_{\boldsymbol{r}} + \frac{e}{m}\boldsymbol{E}\cdot\nabla_{\boldsymbol{c}}\right] f(\boldsymbol{r},\boldsymbol{c},t) = -J(f,f_0), \quad (1)$$

where ∂_t, ∇_r and ∇_c are the gradients with respect to time, space and velocity, while e and m are the charge and mass of the positron and E is the magnitude of the electric field. The right-hand side of equation (1) $J(f,f_0)$ denotes the linear positron-neutral molecule collision operator, accounting for elastic, inelastic and nonconservative (e.g. Ps formation and/or annihilation) collisions. For elastic collisions we use the original Boltzmann collision operator [53], while for inelastic collisions we prefer the semiclassical generalization of Wang-Chang et al. [54]. The collision operators for non-conservative collisions are discussed in [55,56].

The solution of equation (1) is found by expanding $f(\boldsymbol{r},\boldsymbol{c},t)$ as sums of products with the directional dependence of $\boldsymbol{c}$ contained in spherical harmonics $Y_m^{[l]}(\hat{\boldsymbol{c}})$, the spatial distribution contained in $G_\mu^{(s\lambda)}$, the sth application of the spatial gradient operator on $n(\boldsymbol{r},t)$, and the speed distribution contained in an expansion discussed below. Thus, we have:

$$f(\boldsymbol{r},\boldsymbol{c},t) = \sum_{l=0}^{\infty}\sum_{m=-l}^{l}\sum_{s=0}^{\infty}\sum_{\lambda=-s}^{s} f(lm|s\lambda;c)\, Y_m^{[l]}(\hat{\boldsymbol{c}}) G_m^{(s\lambda)}. \quad (2)$$

The coefficients $f(lm|s\lambda;c)$ are functions of the speed c, obtained by the expansion

$$f(lm|s\lambda;c) = \omega(\alpha,c)\sum_{\nu'=0}^{\infty} F(\nu lm|s\mu;\alpha)\, R_{\nu' l}(\alpha,c), \quad (3)$$

where

$$\omega(\alpha,c) = \left(\frac{\alpha^2}{2\pi}\right)^{3/2}\exp\left\{\frac{-\alpha^2c^2}{2}\right\}, \quad (4)$$

$$\alpha^2 = \frac{m}{kT_b}, \quad (5)$$

$$R_{\nu l}(\alpha c) = N_{\nu l}\left(\frac{\alpha c}{\sqrt{2}}\right)^l S_{l+1/2}^{(\nu)}\left(\frac{\alpha^2c^2}{2}\right), \quad (6)$$

$$N_{\nu l}^2 = \frac{2\pi^{2/3}\nu!}{\Gamma(\nu+l+3/2)}, \quad (7)$$

and $S_{l+1/2}^{(\nu)}(\alpha^2c^2/2)$ are Sonine polynomials.

Using the orthonormality conditions of the spherical harmonics and modified Sonine polynomials, the following hierarchy of kinetic equations follows:

$$\sum_{\nu'=0}^{\infty}\sum_{l'=0}^{\infty}\Big[\partial_t\delta_{\nu\nu'}\delta_{ll'} + n_0 J_{\nu\nu'}^{l}(\alpha)\delta_{ll'} - R_a\delta_{\nu\nu'}\delta_{ll'} + ia\alpha(l'm10|lm)\langle\nu l||K^{[1]}||\nu' l'\rangle - n_0 J_{0\nu'}^{0}(\alpha)F(\nu l0|00;\alpha)\times(1-\delta_{s0}\delta_{\lambda0})\delta_{l'0}\delta_{m0}\Big]F(\nu' lm|s\lambda;\alpha) = X(\nu lm|s\lambda;\alpha), \quad (8)$$

where R_a is the rate for Ps formation. The reduced matrix elements of the collision operator $J_{\nu\nu'}^{l}(\alpha)$ and velocity derivative $\langle\nu l||K^{[1]}||\nu' l'\rangle$ are defined by equations (11) and (12) given in reference [56] while $(l'm10|lm)$ is a Clebsch-Gordan coefficient. The explicit expression for the RHS are given in references [37,56].

The hierarchy of kinetic equations (8) is solved by truncation of the ν and l indices to $\nu_{\max}$ and $l_{\max}$, respectively. These values are independently increased until the desired convergence is obtained. T_b is not equal to the neutral gas temperature (the two-temperature method) and is used as a free parameter to optimize the convergence. After truncation, we have a hierarchy of coupled complex equations. This sparse system of equations is solved using standard sparse inversion routines.

The "two term" approximation is based upon the choice of setting the upper bound on the summation in (2) to $l_{max} = 1$ and formed the basis for the classical theory of light charged particle transport properties. It is entirely inappropriate when the distribution function deviates substantially from isotropy in velocity space, and this is exactly what may happen for positrons in CF_4. In Section 4.2.4 we study the convergence trend for various transport coefficients as a function of E/n_0 for positrons in CF_4.

3.1 Transport properties

The transport coefficients of interest (rate coefficient for Ps formation k_{Ps}; bulk drift velocity W; longitudinal (D_L) and transverse (D_T) diffusion coefficients) are related to

the calculated moments via

$$k_{Ps} = n_0 \sum_{\nu'=0}^{\infty} J^0_{0\nu'}(\alpha) F(\nu' 00|00), \tag{9}$$

$$W = \frac{i}{\alpha} F(010|00) - i n_0 \sum_{\nu'=1}^{\infty} J^0_{0\nu'}(\alpha) F(\nu' 00|11), \tag{10}$$

$$D_L = -\frac{1}{\alpha} F(010|11) - n_0 \sum_{\nu'=0}^{\infty} J^0_{0\nu'} \left[F(\nu' 00|20) - \sqrt{2} F(\nu' 00|22) \right], \tag{11}$$

$$D_T = -\frac{1}{\alpha} F(011|11) - n_0 \sum_{\nu'=0}^{\infty} J^0_{0\nu'} \left[F(\nu' 00|20) + \frac{1}{\sqrt{2}} F(\nu' 00|22) \right], \tag{12}$$

where the components involving summations constitute the explicit effects of Ps formation on the transport coefficients, while the remainders constitute the flux contribution.

The spatially homogeneous mean energy ε and gradient energy vector $\boldsymbol{\gamma}$, defined through a density gradient expansion of the averaged positron energy $\epsilon(\boldsymbol{r}, t)$

$$\epsilon(\boldsymbol{r}, t) = \frac{1}{n(\boldsymbol{r}, \boldsymbol{t})} \int \frac{1}{2} m c^2 f(\boldsymbol{r}, \boldsymbol{c}, t)\, d\boldsymbol{c} = \varepsilon + \gamma \cdot \frac{\nabla n}{n} + \ldots, \tag{13}$$

play a pivotal role in a qualitative understanding of the effects associated with the explicit influence of Ps formation on the positron drift and diffusion. The gradient energy parameter $\boldsymbol{\gamma}$ describes the first order spatial variation of the average energy through the positron swarm. These quantities are given by:

$$\varepsilon = \frac{3}{2} k T_b \left[1 - \sqrt{\frac{2}{3}} F(100|00) \right],$$
$$\gamma = \frac{3}{2} k T_b \left[i \sqrt{\frac{2}{3}} F(100|11) \right]. \tag{14}$$

The components of the temperature tensor perpendicular and parallel to the electric field are, respectively:

$$T_T = T_b \left[1 - \sqrt{\frac{2}{3}} F(100|00;\alpha) + \sqrt{\frac{1}{3}} F(020|00;\alpha) \right], \tag{15}$$

$$T_L = T_b \left[1 - \sqrt{\frac{2}{3}} F(100|00;\alpha) - \frac{2}{\sqrt{3}} F(020|00;\alpha) + F(010|00;\alpha)^2 \right]. \tag{16}$$

Ratio between transverse T_T and longitudinal T_L elements of the temperature tensor is usually used as a measure of thermal anisotropy which reflects the anisotropy of the distribution function in velocity space, as discussed below.

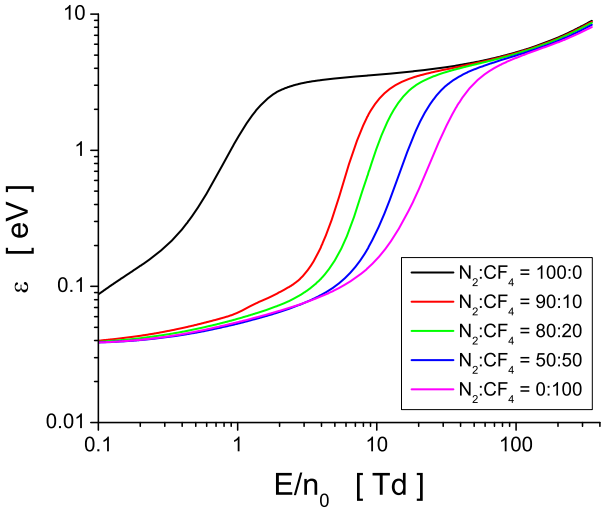

Fig. 2. Variation of the mean energy with E/n_0 in N_2/CF_4 mixture.

4 Results and discussion

4.1 Preliminaries

As discussed in Sections 2 and 3, the aim of this work is to determine positron transport properties in mixtures of N_2 and CF_4. We consider the reduced electric field E/n_0 range: 0.1−350 Td (1 Td = 10^{-21} V m^2). The cross sections for positron scattering in N_2 detailed in our previous papers are used [28].

The results of a multi term solution of Boltzmann's equation are verified with those of an independent Monte Carlo simulation. Our Monte Carlo simulation code has been tested in great details under conditions when the transport of positrons is greatly affected by the Ps formation [26,27,31]. The agreement between results obtained by these two entirely independent techniques is excellent but for the reason of clarity, we show the Boltzmann equation results only.

4.2 Positron transport properties in N_2/CF_4 mixtures

4.2.1 Mean energy of the positrons and rate coefficient for Ps formation

In Figure 2 we show the variation of the mean energy with E/n_0. The properties of the cross sections are reflected in the profiles of the mean energy. We see that the mean energy, as expected, is greatly affected by the addition of CF_4 to N_2. In general, the addition of CF_4 to N_2 decreases the mean energy, and the mean energy curves move to the right and one may view this as a "cooling effect". For pure CF_4 and mixtures of N_2 and CF_4 we see three distinct regions of transport. First, there is a region of slow rise due to large energy losses associated with vibrational excitations. Second, there is a region of sharp rise as the cross sections for vibrational excitations drop off and positrons start to rapidly gain energy from

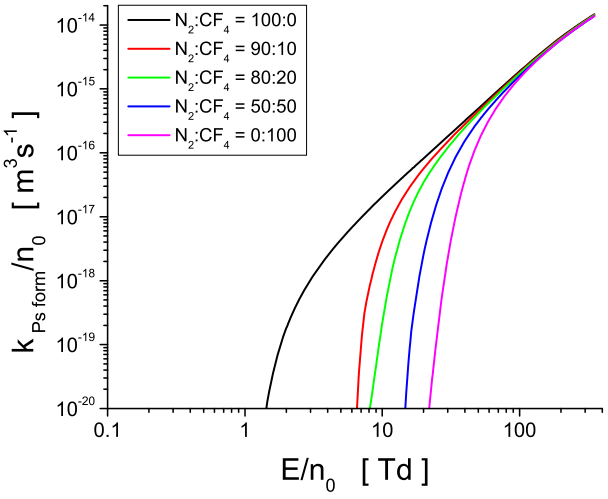

Fig. 3. Variation of the rate coefficient for Ps formation with E/n_0 in N_2/CF_4 mixture.

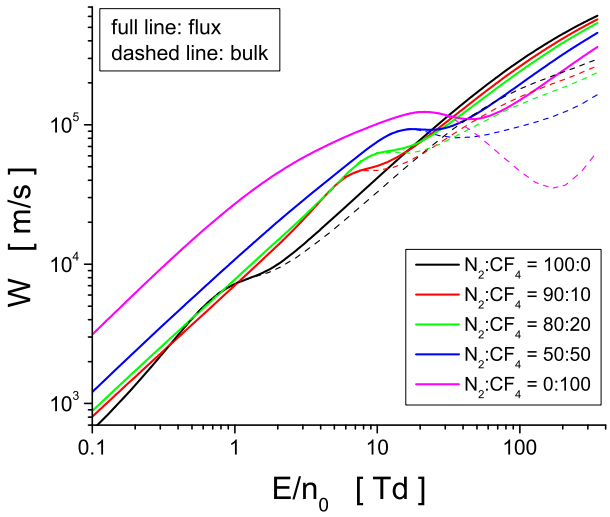

Fig. 4. Variation of the drift velocity with E/n_0 in N_2/CF_4 mixture.

the electric field. Finally, there is another region of slow rise as new inelastic channels including the Ps formation, electronic excitation and direct ionization are open. In the limit of high E/n_0, the mean energy of electrons is relatively insensitive to the gas composition. The same applies for the lowest E/n_0 considered in this work where the mean energy essentially approaches to the thermal value. From Figure 2 we clearly see why CF_4 is such a good addition to N_2 when it comes to thermalizing positrons.

In Figure 3 we display the variation of the rate coefficient for Ps formation with E/n_0. The curves show the expected increase in k_{Ps}/n_0 with E/n_0 and decrease in k_{Ps}/n_0 with increasing fraction of CF_4 in the mixture. For higher E/n_0 k_{Ps}/n_0 shows a weak sensitivity with respect to the composition of the mixture. Note that the values for k_{Ps}/n_0 vary by large orders of magnitude as the reduced electric field E/n_0 is increased from below 10 Td up to 350 Td.

4.2.2 Drift of the positrons and negative differential conductivity

In Figure 4 we show the variation of the flux and bulk drift velocities with the applied reduced electric field E/n_0. A prominent feature of the pure CF_4 and mixtures where the fraction of N_2 is approximately less than 50% is the presence of a region of negative differential conductivity (NDC). This is the region in which the electron drift velocity decreases for increasing values of E/n_0. The NDC behavior for positrons and conditions leading to this phenomenon have been investigated for a range of gases, including Ar [26], N_2 [30], and H_2 [29] and H_2O [31]. For all gases, except for N_2, the existence of NDC was observed only in the bulk drift velocity component with no signs of the same phenomenon in the profiles of the flux component. This was a clear indication that NDC in these gases is induced by the non-conservative nature of the Ps formation. This conclusion has been confirmed in calculations where the Ps formation was treated as a conservative inelastic process; the NDC phenomenon has been removed from the profiles of the bulk drift velocity along with the differences between bulk and flux drift velocity components.

In pure CF_4, and for mixtures where the fraction of N_2 is approximately less than 50%, the situation is more complex. We see from Figure 4 that both the bulk and flux drift velocities exhibit NDC. However, the origin of NDC is different for the different types of drift velocity. The NDC of the flux component is induced by the shape of cross sections as is observed for electrons in the same gas [47]. Therefore the NDC in the bulk component will also have NDC due to the shape of the cross sections but it may have an additional contribution due to the non-conservative nature of Ps formation. Following the strategy from our previous papers, we have treated Ps formation as a conservative inelastic process. As a consequence, the difference between two drift velocity components was removed but NDC effect was still present in the profiles. From the studies of electron transport in neutral gases, it is well known that NDC arises for certain combinations of elastic and inelastic cross sections in which, on increasing the electric field, there is a rapid transition in the dominant energy loss mechanism from inelastic to elastic [57,58]. The determining factor is how rapidly the ratio of the inelastic to elastic cross sections falls with the increasing mean energy/applied field. Typically, the effect is enhanced by (i) a rapidly increasing cross section for elastic collisions and/or (ii) a rapidly decreasing inelastic cross section. In the transition regime, the enhanced randomization of the directed motion decreases the drift velocity even though the mean energy increases. From Figure 4, for pure CF_4 we see that NDC occurs between approximately 20 and 50 Td, where the mean energies are between 0.4 and 3 eV. It is exactly in this energy range that the combination of a rapidly increasing cross section for elastic collisions and a rapidly decreasing cross section for vibrational

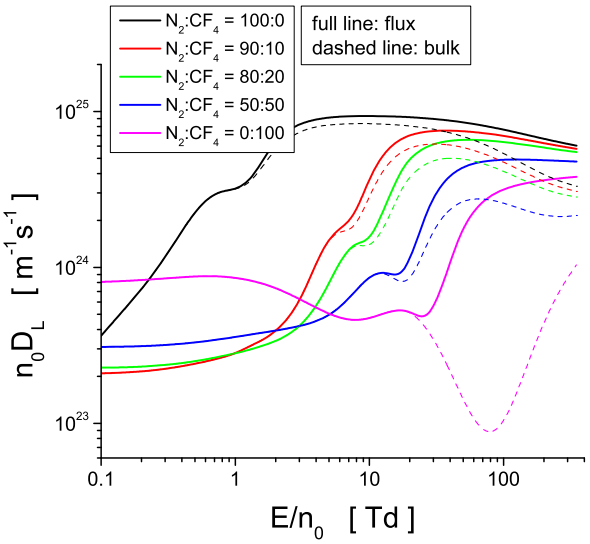

Fig. 5. Variation of the longitudinal diffusion coefficient with E/n_0 in N_2/CF_4 mixture.

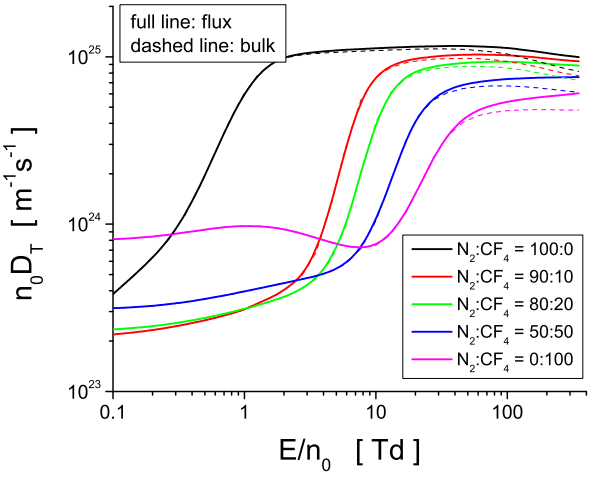

Fig. 6. Variation of the transverse diffusion coefficient with E/n_0 in N_2/CF_4 mixture.

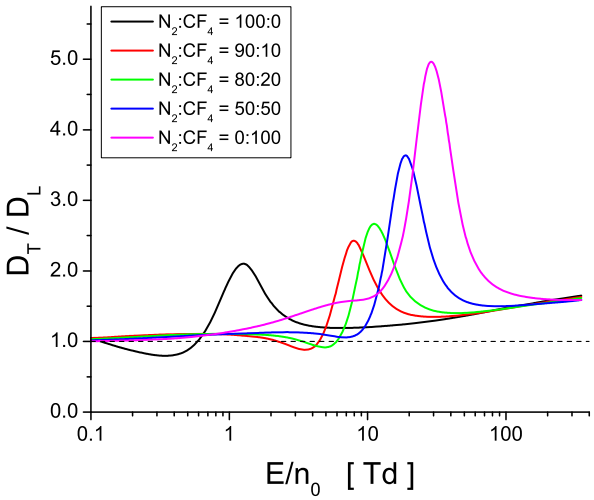

Fig. 7. Variation of the ratio between transverse and longitudinal diffusion coefficients with E/n_0 in N_2/CF_4 mixture.

excitation in the region of the Ramsauer-Townsend minimum in CF_4 occurs which favours the development of NDC. It is clear that complexity of NDC phenomenon in CF_4 follows directly from the complex energy dependence of the cross sections for positron scattering.

4.2.3 Diffusion of the positrons

In Figures 5 and 6 we show the variation of the longitudinal and transverse diffusion coefficients with E/n_0. In general, it is hard to fully understand the behavior of diffusion coefficients even in pure electric field since many parallel factors affect them simultaneously. In addition to the effects of thermal anisotropy (dispersion of positrons due to thermal motion is not the same in different directions) and electric anisotropy (spatial variation of the average energy in conjunction with energy-dependent collision frequency produces differences in the average local velocities for a given direction, which act to inhibit and/or enhance diffusion in that direction), there is always the contribution of collisions and the complex energy dependence of Ps formation that even further complicate the physical picture.

Both the bulk and flux data are shown in Figures 5 and 6 with the aim of determining how sensitive diffusion is on the presence of Ps formation. First, for both n_0D_L and n_0D_T and for all mixtures we see that the bulk data are dominated by the corresponding flux data. The addition of CF_4 to N_2 increases the differences between the bulk and flux for n_0D_L while the differences between the bulk and flux for n_0D_T remain essentially unaltered. The transverse diffusion coefficient appears in general to be less sensitive to the effects of Ps formation than the longitudinal diffusion coefficient. On the other hand, for pure CF_4 around 100 Td, we observe deviations of more than one order of magnitude between the flux and bulk for n_0D_L which is another important manifestation of the explicit non-conservative effects of the Ps formation processes. To study in detail the explicit effects of Ps formation on the diffusion coefficients, a comprehensive investigation of the spatially resolved data along the swarm, particularly those associated with the second-order variations of the average energy is required. This is beyond the scope of this paper and we defer the detailed discussion on the explicit influence of Ps formation on diffusion processes for positrons in mixtures of N_2 and CF_4 to a future paper.

In Figure 7 we show the variation of the ratio between the flux transverse and flux longitudinal diffusion coefficients with E/n_0. The differences between the longitudinal and transverse diffusion coefficients is evidence of the anisotropic nature of diffusion which generally follows from the interplay of energy dependent collision frequency and spatial variation of average energy along the swarm. We see that the anisotropic nature of the diffusion is enhanced as the fraction of CF_4 is increased. Since

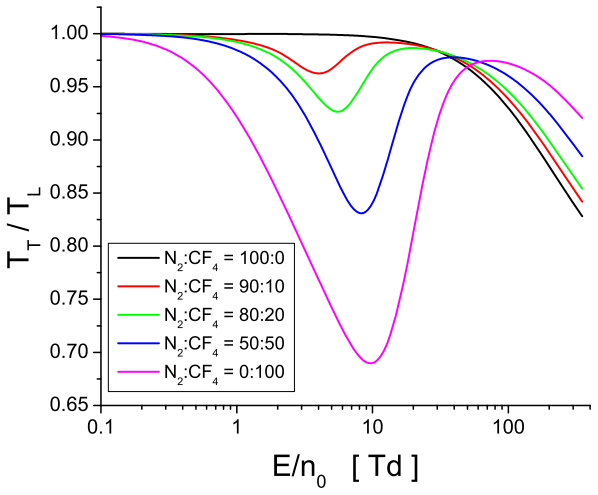

Fig. 8. Variation of the ratio between transverse and longitudinal components of the temperature tensor with E/n_0 in N_2/CF_4 mixture.

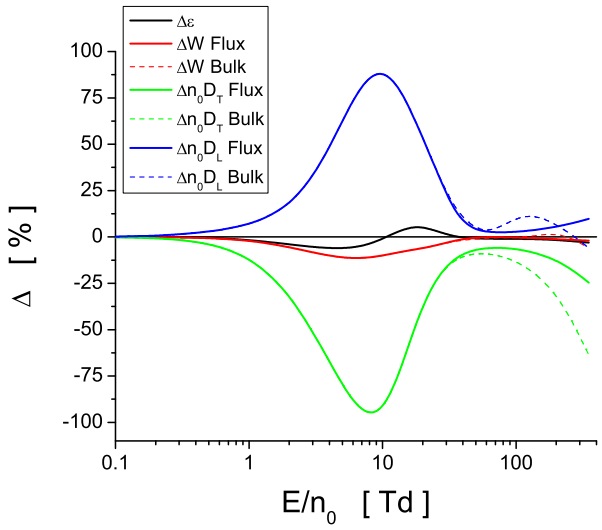

Fig. 9. Percentage difference between the two term and multi term results for the mean energy, drift velocity and diffusion coefficients for positrons in CF_4.

the average energy increases along the swarm for all mixtures and for all applied reduced electric fields (as checked in our independent Monte Carlo simulations), it then follows that for pure CF_4 and mixtures where the fraction of N_2 is less than 50% the total collision frequency is a monotonically increasing function of the positron energy. For pure N_2 and mixtures where the fraction of CF_4 is dominated by the fraction of N_2, we see that for a certain range of E/n_0 the opposite situation holds: n_0D_L dominates n_0D_T indicating a decrease of the total collision frequency with the positron energy in the same region. It is interesting to note that the values of the reduced electric field, $(E/n_0)_{\max}$, for which the ratio between n_0D_L and n_0D_T reaches a local maximum are shifted to higher fields, and that this is not linear with increasing fraction of CF_4. It should be noted that the anisotropy of the bulk diffusion tensor is almost the same for all mixtures except for pure CF_4 where there is a strong reduction of the bulk longitudinal diffusion coefficient induced by the explicit effects of Ps formation.

4.2.4 The two term vs. multi term results

In Figure 8 we display the variation of the ratio between the transverse and longitudinal components of the temperature tensor with E/n_0. The anisotropy of the temperature tensor reflects the anisotropy of the distribution function in velocity space and a knowledge of its variation with E/n_0 is of essential importance for studies associated with the accuracy of the two term approximation for solving the Boltzmann equation for positrons in neutral gases [29]. We observe that the anisotropy of the temperature tensor is significantly increased for increasing fractions of CF_4 in CF_4/N_2 mixtures. The fields at which the T_T/T_L profiles are a minimum correspond approximately to those where the maximum error in the two term approximation occurs.

In Figure 9 we display the percentage difference between the two term and fully converged results for the mean energy, drift velocity and diffusion coefficients in pure CF_4. Truncation at $l_{\max} = 6$ was required to achieve convergence to within 1% for all transport coefficients and properties. We observe that the mean energy and drift velocity can be in error by approximately 10% while the diffusion coefficients can have errors of the order of 100%. We see that the maximum error in the two term approximation, for all three transport coefficients occurs at about 5−10 Td. In this field region, the mean energy ε is in the range 0.1−0.2 eV, and from the plot of cross section shown in Figure 1 it is evident that at this energy the cross section for elastic collisions is almost at a minimum and the vibrational excitation processes become significant. This combined effect produces a large asymmetry in velocity space which makes the two term approximation inadequate for the analysis of positron transport data. As the cross section for elastic collisions increases rapidly with energy beyond the minimum, a decrease in the error of the two term approximation is observed in Figure 9. For higher fields, due to the influence of other inelastic channels, the accuracy of two term approximation again deteriorates, particularly for the diffusion coefficients.

5 Conclusion

In this paper we have presented an essentially complete set of scattering cross sections for positron in CF_4. Cross sections have been compiled from the best available data from the literature and modified using physical arguments. The main features are very large cross sections for vibrational excitations in the region of Ramsauer-Townsend minimum for elastic collisions, and a huge cross section for Ps formation exhibiting a strong energy dependence. If one wants to improve the current set of cross section for positron

scattering in CF_4, then further measurements of positron swarm data are needed, including drift velocity, diffusion coefficients and rate coefficient for Ps formation. In addition, more studies of electronic excitation and dissociation are required in order to refine and normalize the existing set of cross sections. However, this set of cross sections should be sufficient for modeling of positron traps.

In addition to the collisional data, using a multi term theory for solving the Boltzmann equation, we have calculated positron transport properties, including the mean energy, drift velocity and diffusion coefficients as well as rate coefficient in pure CF_4 and CF_4/N_2 mixtures. Calculations have been performed under conditions critical for modeling of positron traps, and we have focussed on the way in which the positron transport properties are influenced by the explicit effects of Ps formation. The following important points have been observed: (i) the addition of CF_4 to N_2 decreases the mean energy and cools down the positrons; (ii) NDC phenomenon has been observed in the profiles of both the bulk and flux drift velocity; (iii) the longitudinal diffusion coefficients is more sensitive than the transverse diffusion coefficient with respect to the Ps formation; and (iv) from the profiles of the diagonal elements of the temperature tensor we have concluded that the distribution function in velocity space is highly anisotropic for certain range of the reduced electric fields which makes the two term approximation for solving the Boltzmann equation inadequate for the analysis of positron transport data.

This work was supported by MPNTRS Projects ON171037 and III41011, and Australian Research Council. Authors are also grateful to Professors Michael Brunger and James Sullivan for discussions, ideas, and collaboration on some of the topics presented here.

References

1. M. Charlton, J. Humberston, *Positron Physics* (Cambridge University Press, New York, 2000)
2. F. Gribakin, H. Knudsen, C.M. Surko, Phys. Scr. **70**, C1 (2004)
3. M.W.J. Bromley, M.A.P. Lima, G. Laricchia, Phys. Scr. **74**, C37 (2006)
4. G. Muehllehner, J.S. Karp, Phys. Med. Biol. **51**, R117 (2006)
5. N. Guessoum, R. Ramaty, R.E. Lingenfelter, ApJ **378**, 170 (1991)
6. L.D. Hulett Jr., D.L. Donohue, J. Xu, T.A. Lewis, S.A. McLuckey, G.L. Glish, Chem. Phys. Lett. **216**, 236 (1993)
7. R.M. Moadel, A.V. Nguyen, E.Y. Lin, P. Lu, J. Mani, M.D. Blaufox, J.W. Pollard, E. Dadacheva, Breast Cancer Res. **5**, 199 (2003)
8. R.M. Moadel, R.H. Weldon, E.B. Katz, P. Lu, J. Mani, M. Stahl, M.D. Blaufox, R.G. Pestell, M.J. Charron, E. Dadachova, Cancer Res. **65**, 698 (2005)
9. M. Charlton, J. Phys.: Conf. Ser. **162**, 012003 (2009)
10. Z.Lj. Petrović, A. Banković, S. Dujko, S. Marjanović, M. Suvakov, G. Malović, J.P. Marler, S.J. Buckman, R.D. White, R.E. Robson, J. Phys.: Conf. Ser. **199**, 012016 (2010)
11. C.M. Surko, A. Passner, M. Leventhal, F.J. Wysoki, Phys. Rev. Lett. **61**, 1831 (1988)
12. T.J. Murphy, C.M. Surko, Phys. Rev. A **46**, 5696 (1992)
13. J.P. Sullivan, S.J. Gilbert, J.P. Marler, R.G. Greaves, S.J. Buckman, C.M. Surko, Phys. Rev. A **66**, 042708 (2002)
14. J.P. Marler, J.P. Sullivan, C.M. Surko, Phys. Rev. A **71**, 022701 (2005)
15. A.C.L. Jones, C. Makochekanwa, P. Caradonna, D.S. Slaughter, J.R. Machacek, R.P. McEachran, J.P. Sullivan, S.J. Buckman, A.D. Stauffer, I. Bray, D.V. Fursa, Phys. Rev. A **83**, 032701 (2011)
16. J.P. Sullivan, C. Makochekanwa, A. Jones, P. Caradonna, S.J. Buckman, J. Phys. B **41**, 081001 (2008)
17. C. Makochekanwa, O. Sueoka, M. Kimura, J. Phys.: Conf. Ser. **80**, 012012 (2007)
18. C.M. Surko, R.G. Greaves, Phys. Plasmas **11**, 2333 (2004)
19. J. Clarke, D.P. van der Werf, B. Griffiths, D.C.S. Beddows, M. Charlton, H.H. Telle, P.R. Watkeys, Rev. Sci. Instrum. **77**, 063302 (2006)
20. J.P. Sullivan, A. Jones, P. Caradonna, C. Makochekanwa, S.J. Buckman, Rev. Sci. Instrum. **79**, 113105 (2008)
21. D.B. Cassidy, S.H.M. Deng, R.G. Greaves, A.P. Mills, Rev. Sci. Instrum. **77**, 073106 (2006)
22. G.B. Andresen et al., Nature **468**, 673 (2010)
23. M. Amoretti et al., Nature **419**, 456 (2002)
24. G. Gabrielse et al., Phys. Rev. Lett. **89**, 213401 (2002)
25. D.B. Cassidy, V.E. Meligne, A.P. Mills Jr., Phys. Rev. Lett. **104**, 173401 (2010)
26. M. Suvakov, Z.Lj. Petrović, J.P. Marler, S.J. Buckman, R.E. Robson, G. Malović, New J. Phys. **10**, 053034 (2008)
27. J.P. Marler, Z.Lj. Petrović, A. Banković, S. Dujko, M. Suvakov, G. Malović, S.J. Buckman, Phys. Plasmas **16**, 057101 (2009)
28. A. Banković, J.P. Marler, M. Suvakov, G. Malović, Z.Lj. Petrović, Nucl. Instrum. Methods Phys. Res. B **266**, 462 (2008)
29. A. Banković, S. Dujko, R.D. White, S.J. Buckman, Z.Lj. Petrović, Nucl. Instrum. Methods Phys. Res. B **279**, 92 (2012)
30. A. Banković, Z.Lj. Petrović, R.E. Robson, J.P. Marler, S. Dujko, G. Malović, Nucl. Instrum. Methods Phys. Res. B **267**, 350 (2009)
31. A. Banković, S. Dujko, R.D. White, J.P. Marler, S.J. Buckman, S. Marjanović, G. Malović, G. García, Z.Lj. Petrović, New J. Phys. **14**, 035003 (2012)
32. S. Marjanović, M. Suvakov, A. Banković, M. Savić, G. Malović, S.J. Buckman, Z.Lj. Petrović, IEEE Trans. Plasma Sci. **39**, 2614 (2011)
33. S. Marjanović, M. Šuvakov, A. Banković, Z.Lj. Petrović, submitted to Phys. Rev. A
34. J.P. Marler, C.M. Surko, Phys Rev. A **72**, 062713 (2005)
35. A.V. Phelps, K. Tachibana, private communication
36. A. Banković, Z.Lj. Petrović, R.E. Robson, J.P. Marler, S. Dujko, G. Malović, Nucl. Instrum. Methods Phys. Res. B **267**, 350 (2009)
37. S. Dujko, R.D. White, Z. Lj. Petrović, R.E. Robson, Phys. Rev. E **81**, 046403 (2010)
38. S. Dujko, R.D. White, Z.Lj. Petrović, R.E. Robson, Plasma Source Sci. Technol. **20**, 024013 (2011)
39. Y. Itikawa, N. Mason, J. Phys. Chem. Ref. Data **34**, 1 (2005)
40. Z.Lj. Petrović, A. Banković, S. Dujko, S. Marjanović, G. Malović, J.P. Sullivan, S.J. Buckman, AIP Conf. Proc. **1545**, 115 (2013)

41. R.G. Greaves, C.M. Surko, Nucl. Instrum. Methods Phys. Res. B **192**, 90 (2002)
42. T. Nishimura, F.A. Gianturco, J. Phys. B **37**, 215 (2004)
43. J. Moxom, D.M. Schrader, G. Laricchia, J. Xu, L.D. Hullet, Phys. Rev. A **62**, 052708 (2000)
44. H. Bluhme, Ph.D. Thesis, University of Aarhus, 2000
45. L.G. Christophorou, J.K. Olthoff, Appl. Surf. Sci. **192**, 309 (2002)
46. J. Tennyson, private communication
47. M. Kurihara, Z.Lj. Petrović, T. Makabe, J. Phys. D **33**, 2146 (2000)
48. G.G. Raju, *Gaseous Electronics: Theory and Practice* (CRC Press Taylor & Francis, Boca Raton, 2006)
49. K.P. Huber, G. Herzberg, in *Molecular Spectra and Molecular Structure* (Van Nostrand Reinhold Company, New York, 1979), Vol. 4
50. L.G. Christophorou, J.K. Olthoff, M.V.V.S. Rao, J. Phys. Chem. Ref. Data **25**, 1341 (1996)
51. L.G. Christophorou, J.K. Olthoff, J. Phys. Chem. Ref. Data **28**, 967 (1999)
52. M.T. do N. Varella, A.P.P. Natalense, M.H.F. Bettega, M.A.P. Lima, Phys. Rev. A **60**, 3684 (1999)
53. L. Boltzmann, Wein. Ber. **66**, 275 (1872)
54. C.S. Wang-Chang, G.E. Uhlenbeck, J. DeBoer, in *Studies in Statistical Mechanics*, edited by J. DeBoer, G.E. Uhlenbeck (Wiley, New York, 1964), Vol. 2, p. 241
55. R.E. Robson, K.F. Ness, Phys. Rev. A **33**, 2086 (1986)
56. K.F. Ness, R.E. Robson, Phys. Rev. A **34**, 2185 (1986)
57. Z.Lj. Petrović, R.W. Crompton, G.N. Haddad, Aust. J. Phys. **37**, 23 (1984)
58. R.E. Robson, Aust. J. Phys. **37**, 35 (1984)